Ultrafast Ge-Te bond dynamics in a phase-change superlattice

Marco Malvestuto,[1, *] Antonio Caretta,[1] Barbara Casarin,[2, 1] Federico Cilento,[1] Martina Dell'Angela,[1] Daniele Fausti,[2] Raffaella Calarco,[3] Bart J. Kooi,[4] Enrico Varesi,[5] John Robertson,[6] and Fulvio Parmigiani[2, 1, 7]

[1] *Elettra-Sincrotrone Trieste S.C.p.A. Strada Statale 14 - km 163.5 in AREA Science Park 34149 Basovizza, Trieste, Italy*
[2] *Department of Physics, University of Trieste, Via A. Valerio 2, 34127 Trieste, Italy*
[3] *Paul-Drude-Institut für Festkörperelektronik, Hausvogteiplatz 5-7, 10117 Berlin, Germany*
[4] *Zernike Institute for Advanced Materials, University of Groningen, Groningen, 9747 AG, The Netherlands*
[5] *Micron Semiconductor Italia S.r.l., Via C. Olivetti, 2, 20864, Agrate Brianza, MB, Italy*
[6] *Engineering Department, Cambridge University, Cambridge CB2 1PZ, UK*
[7] *International Faculty, University of Cologne, 50937 Cologne, Germany*

A long-standing question for avant-grade data storage technology concerns the nature of the ultrafast photoinduced phase transformations in the wide class of chalcogenide phase-change materials (PCMs). Overall, a comprehensive understanding of the microstructural evolution and the relevant kinetics mechanisms accompanying the out-of-equilibrium phases is still missing. Here, after overheating a phase-change chalcogenide superlattice by an ultrafast laser pulse, we indirectly track the lattice relaxation by time resolved X-ray absorption spectroscopy (tr-XAS) with a sub-ns time resolution. The novel approach to the tr-XAS experimental results reported in this work provides an atomistic insight of the mechanism that takes place during the cooling process, meanwhile a first-principles model mimicking the microscopic distortions accounts for a straightforward representation of the observed dynamics. Finally, we envisage that our approach can be applied in future studies addressing the role of dynamical structural strain in phase-change materials.

I. INTRODUCTION

In these last years innovative fields for cutting-edge technologies based on novel engineered materials have been disclosed by the understanding of the non-equilibrium optical control of the matter.

For instance the comprehension of the non-equilibrium mechanisms is of paramount importance for exploiting the physical and optical properties of the phase-change materials (PCMs), nowadays used in optical data storage[1] and non-volatile electrical memories[2].

The key feature of these intriguing compounds is the large and steep change of the optical and electrical properties observed when comparing the covalent bonded amorphous phase with the resonantly bonded crystalline phase. Interestingly, this scenario has been recently enriched by the chalcogenide superlattice (CSL), that are regarded as novel phase-change materials[3,4], where the phase transition is between two crystalline structures, rather than amorphous to crystalline or vice-versa.

However, it is stimulating the fact that all these materials share common phase change properties, such as the switching time, the activation energy and the dielectric response, hence suggesting that a similar physics must govern the complex nature of their local atomic structure and configuration conditions.

To shed light on these compelling mechanisms, some models, based mainly on thermal or electronic processes, have been proposed.[5–16]

Conversely, other studies[17–22] suggest that more complex mechanisms are governing the atomic dynamics at the base of the phase switching, where concomitant thermal and electronic aspects compete in a synergic feedback loop[17]. Yet, the structural dynamics during fast temperature quenching processes of overheated GSTs glasses

and crystals is still unclear.[8,9] Indeed, when the heating-cooling cycle between two structural phases is closely observed, a variety of parameters (from quenching velocity to thermal dissipation and/or structural strain)[23] dictate the out-of-equilibrium dynamical evolution in the energy phase space across either the amorphous-crystal or the crystalline-crystalline phase transformation[24]. Henceforth, the role of the quenching processes on the final structural configuration may not simply be a thermal dissipation, especially when the cooling rate are in the range of 10^{12}K/s or the heating stimulus is intense and ultrafast, i.e. in the ps time range. These considerations indicates that a comprehensive knowledge of the cooling phase in GSTs is paramount.

Scope of this work is thus to assess the role of the ultrafast thermal strain dynamics in a CSL structure during the first instants of the heating-cooling cycle. To this end, we cyclically heat a CSL sample slightly below its phase change temperature and observe the cooling phase by means of time-resolved X-ray absorption spectroscopy (tr-XAS) of the Ge-L$_3$ edge. By mean of first-principles multiple scattering simulations for interpreting tr-XAS experiments, we unveil the microscopic structural and the dynamical changes occurring after the ultrafast heating of a nominal [GeTe(1nm)/Sb$_2$Te$_3$(3nm)]$_{15}$ CSL. The present results allow to unambiguously ascribe the distinct features of tr-XAS spectra to the dynamical structural strain occurring during the thermal quenching process.

Recently, Ge L$_3$-edge XAS of GeTe based alloys[25,26] have been interpreted using real-space *ab-initio* multiple scattering simulations on crystalline and amorphous models. These and previous[27] studies have confirmed the effectiveness of the Ge L$_3$-edge as a spectroscopic probe to distinguish changes of the local atomic and elec-

tron charge distribution around the Ge photo-absorber. Therefore, by extending the Ge L_3 absorption edge measurement to the time domain, unprecedented details about the local atomic structural dynamics during out-of-equilibrium states, like pre-melting phases and fast cooling processes, could be accessed. In addition, unlike X-ray diffraction, tr-XAS can be applied to both the crystalline and amorphous phases providing a unique information about the projected density of states (pDOS).

II. EXPERIMENT

In the present experiment we probe an as-grown [GeTe(1nm)/Sb$_2$Te$_3$(3nm)]$_{15}$CSL, which has been grown on the Sb-passivated surfaces of Si(111), $(\sqrt{3} \times \sqrt{3})$R30°-Sb, at a substrate temperature of 230 °C, and capped with terminal layer for preventing oxidation[28,29]. The experiments have been carried out at the beamline BACH of the Elettra Synchrotron light source in Trieste, Italy, which operates an optical pump and X-ray probe technique capable of performing tr-XAS experiments with sub-nanosecond time resolution, hence making possible the direct observation of the structural evolution on ultrafast time scales. A general description of the setup is reported elsewhere[30]. In its standard multi-bunch operating mode, the Elettra storage ring delivers X-ray pulses with: (i) low intensity ($\sim 10^3$ photons/pulse in a quasi-monochromatic beam), (ii) high repetition rate (500 MHz) and (iii) a $\sim$100 ps full-width-half-maximum (FWHM) photon pulse temporal profile. This last parameter dictates the maximum time resolution of this experimental scheme. A Ti-sapphire amplified laser source operating at $\sim$233 kHz repetition rate and synchronized with the storage ring radio frequency is used and delivers pump pulses of up to 50 fs pulses at 800 nm, with an energy/pulse of $\sim$6 µJ. The time jitter of the laser with respect to the X-ray pulses is less then 5 ps, while the other relevant laser parameters are reported in Table I. The absorbed energy per pulse is calculated by measuring the sample transmittance response[31] in the 0.1-1 eV energy range and extrapolating the response function value at 1.55 eV (see discussion in Supplemental Material[32] paragraph I).

A simplified sketch of the experimental pump-probe configuration is represented in panel (a) of Fig. 1. The laser is focused on the sample by a 300 mm focal-length lens. Spatial overlap between X-ray and laser pulses is

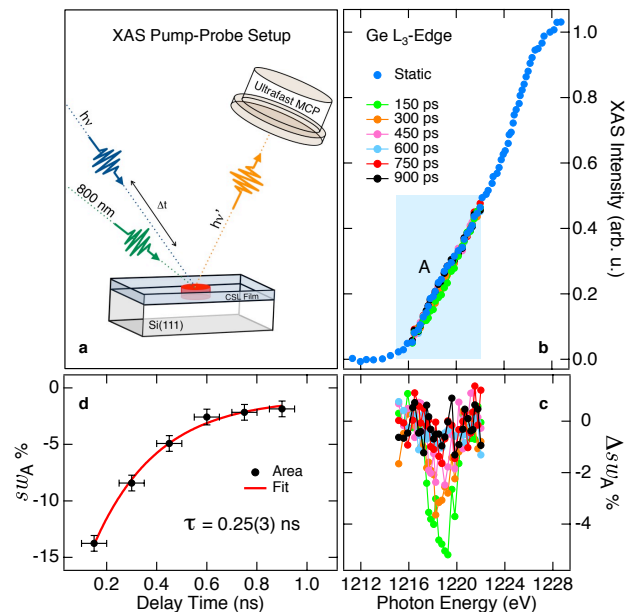|			
Average power	400	mW	
Wavelength (λ)	800	nm	
Spot size	250	µm	
absorbed energy/pulse	0.75	µJ	see SI

TABLE I: Laser parameters

FIG. 1: (Color online) Panel (a) reports a simplified sketch of the setup: the 800 nm laser beam and the synchrotron X-ray pulses, synchronized with delay Δt, are both impinging on a CSL film grown on a Si substrate. Panel (b) shows a collection of Ge L_3 edges taken at different time delays with time step $\delta t \sim$150 ps, in comparison with a static Ge L_3 lineshape (dotted blue curve). Panel (c) shows a close-up of the shoulder A in the ΔE=[1215-1220 eV] photon energy range (blue rectangle in panel (b)) plotted as Δsw$_A$(t) (see text). Panel (d): temporal dynamics of the spectral weight sw$_A$(t) (black dots, see text) fitted with a single exponential function.

ensured by alignment of both pump and probe beams using a 100 µm pinhole[30].

The time resolved XAS Ge L_3-edge was probed in fluorescence mode using an Hamamatsu ultra-fast µ-channel plate[30] and acquired as a function of laser pulse time delay δt. The temporal overlapping of the pump and probe pulses defines the zero time delay (δt=0). The dynamics is measured in 150 ps time delay steps from t=-150 ps to t=900 ps for an overall time interval Δt of $\sim$1 ns.

III. RESULTS AND DISCUSSION

Fig.1(b) reports a near edge region of the Ge L_3-edge lineshape (blue dotted curve) measured across the 2p$_{3/2}$-sp absorption transition ($\sim$ 1220 eV).

The onset of the absorption edge is reported at equilibrium, i.e. without shining laser light on the sample, and after the pre-edge background removal and post-edge normalisation.

A tiny spectral bump A appears at the onset of the absorption threshold in the low energy region (blue box in
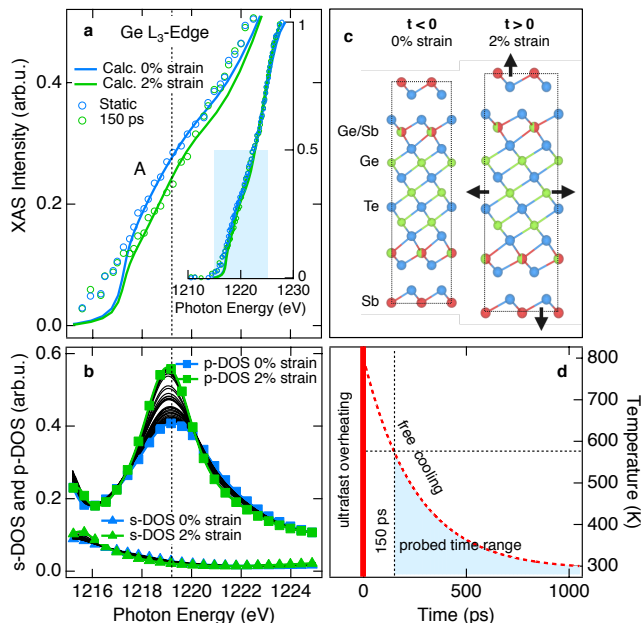
FIG. 2: (Color online) Panel (a) and inset therein: the experimental (open dots) Ge L_3 thresholds measured at time delays $\delta t=0$ (unpumped blue curves) and 150 ps (green dots), respectively, are qualitatively compared to the calculated (continuous curves) Ge L_3 thresholds. The simulated lineshapes have been calculated for no expansion and 2% expansion of the lattice parameters, respectively. Panel (b) displays the Ge 3p- and 4s-DOS curves calculated for a series of strain [(0-2%)] of the crystal lattice. Panel (c) sketches the CSL crystal cell before (equilibrium) and after (heated state) the arrival of the laser pulse. Therein a simplified version of the observed phenomenon is visually represented: the sudden change in temperature drives a lattice expansion of the CSL. The lattice will recover the initial state after complete thermal dissipation is achieved ($T_{in}=T_{fin}$). Panel (d) ΔT calculated through eq. 4.

1(b)) being a direct signature of the specific local atomic Ge-Te coordination and electron charge distribution[26]. The measured photon energy range is limited to about 15 eV around the absorption threshold. In fact, as already reported elsewhere[26] and shown in this work by our calculations, the Ge sp hybridized states, which are responsible of the Ge-Te bonding, are projected over few eVs above the Fermi energy.

Upon laser illumination ($\delta t > 0$), a sudden ($\ll 150$ ps) but small change of the spectral weight of A is observed. Possible sample damaging has been monitored as a function of the laser fluence by acquiring consecutive static Ge L_3 edges and checking for possible changes of the lineshape. The laser fluence used in our work was, in any case, far below the fluencies used in previous works[15,16,33,34].

A collection of representative snapshots of the time evolution of the Ge-L_3 edge as a function of time delay

after the laser excitation is shown superimposed to the equilibrium threshold.

Magnified threshold changes over the bump energy region and time delays are displayed in Fig. 1(c)-(d), where the relative spectral weight change $\Delta sw_A(E)$ (Fig. 1c) and the integrated threshold change $sw_A(t)$ (Fig. 1d) are reported. $\Delta sw_A(E)$ is calculated as the normalized difference between the threshold intensities as a function of δt and of the reference static L_3 edge:

$$\Delta S(E, \delta t) = \frac{S(E, \delta t = 0) - S(E, \delta t)}{S(E, \delta t = 0)}. \qquad (1)$$

$sw_A(t)$ is then calculated by integrating $\Delta sw_A(E)$ over the corresponding energy range:

$$S(t) = \int_{E1}^{E2} \Delta S(E, \delta t)\Delta E. \qquad (2)$$

It can be clearly seen that following the arrival of the laser pump pulse, $\Delta sw_A(E)$ decreases and it reaches its minimum value after the first time delay step of $\sim$150 ps. In addition, considering the temporal evolution of $sw_A(t)$, the initial decrease is followed by its almost complete recovery in about 1 ns.

Since the overall time resolution is limited to the delay step that is comparable with the probe intrinsic time resolution (~ 100ps), spectral changes at shorter delays cannot be appreciated. Hence, the laser excitation and the resulting heating process are too fast to observe.

Ge-L_3 XAS corresponding to either longer or negative time delays confirm that the L_3 shoulder remains unchanged and the measurement is reproducible. This important observation indicates that the material completely recovered the initial state and the impulsive heating-fast cooling cycle is thus reversible.

For the sake of clarity, in the following part of the discussion we will assume that the probed volume of the sample has an average uniform temperature depending δt. Thus temperature inhomogeneities, resulting from the depth dependent heat distribution due to the Beer-Lambert law of light absorption, are neglected. This assumption is validated by considering that the X-ray probe penetration depth at 1.2 KeV is ~ 800 nm[35]. Thus the XAS is providing an averaged information about the local structure. In addition, since the thermal heat dissipation of CSL is relatively high, heat flow smears out the temperature distribution within the probed volume in few ps. It is worth to mention that the CSL/Si interface thermal resistance, which dictates the thermal flow from the CSL film through the bulk Si reservoir, is comparatively higher than the CSL thermal resistance.

The $sw_A(t)$ temporal decay provides information on the dynamics, being $sw_A(t)$ related to both the thermal dissipation and the structural relaxation. Accordingly, by using a one temperature model, the $sw_A(t)$ was fitted with a single exponential function $a \exp^{-\frac{t}{\tau_0}}$, where τ_0 is found to be $\sim$255 ps. The structure then relaxes with

a cooling rate of 10^{12} K/s, which is comparable to that expected for similar glass forming systems[36–38].

Even more interesting is to investigate the role of crystalline structure on the observed spectral changes. Thus, we have computed multiple scattering (MS) simulations[39,40] of the Ge L_3 edge for a series of stretched structures of a known stable structure[28] (displayed in Fig. 2(c) for positive and negative δt), where the unit cell parameters were varied of some tenth of percent (see details in Supplemental Material[32] paragraph IV). Here the assumption, validated by the experimental observation that no phase transition occurs after the absorption of the laser pulse, is that the symmetries of the Ge sites remain unchanged after the laser illumination. The theoretical Ge L_3 XAS spectra shown in Fig. 2 are obtained by averaging the MS XAS lineshape calculated for each Ge crystal site within the CSL unit cell.

In Fig. 2(a) the average Ge L_3 XAS calculated for the undistorted structure and the largest stretched structure are displayed in the close-up energy region of the A bump and they are qualitatively compared with the equilibrium and 150 ps delayed experimental data. The inset of Fig. 2(a) displays the calculated and experimental L_3 spectra over an extended photon energy range. The calculated spectra nicely reproduce the overall experimental lineshapes, while the maximum observable change in time of A is also well reproduced for a maximum 2% lattice expansion.

In Fig. 2(b), the calculated s- and p-symmetry DOSs of Ge are also reported, while d contributions are negligible in this energy range. The p-projected DOSs display a prominent feature peaked at 1219 eV (matching the photon energy range of the feature A in Fig. 1(b)), whose intensity changes as a function of lattice strain. Notably, a tiny change of the s-projected DOSs is also observed, which is consistent with the Ge s-p hybridization.

This phenomenological analysis of the experimental data suggests that the detected changes measured at onset of the Ge L_3 absorption edge, between the sample at equilibrium and after the photoexcitations, i.e. feature A in Fig. 1(b), should originates from lattice strains. This mechanisms is further supported by considering that the bonding overlap between the directional p orbitals of Ge and the first nearest neighbours is strongly affected even by a small lattice expansion/contraction, while the almost spherical s orbitals are only slightly perturbed. On a side note, this observation is also relevant in terms of the ferroelectric properties of the medium, because stretched p-bonds can increase the local electric dipole contribution to the overall polarizability.

Henceforth, consistently with the above scenario, the crystal structure undergoes a sudden lattice expansion corresponding to a fast temperature increase due to the absorption of the ultrafast pump pulse[41]. Then, both the out-of-equilibrium electronic and phonon subsystems and the lattice relax, following the heating thermal dissipation at a cooling rate of 10^{12} K/s (Fig. 2(c-d)).

The average temperature distribution T(t) in the film is calculated from Fourier's law in one dimension, assuming that the electrons and phonons in the system remain in thermal equilibrium. This changing temperature distribution creates a structural strain that can be calculated as

$$\frac{\Delta L}{L} = \delta\sigma = -\alpha_L \delta T \qquad (3)$$

Since any assumption about the strength of the electron-electron and electron-phonon couplings is neglected, it is safe to assume thermal relaxation between the electron and phonon baths[44].

Considering a consistent thermodynamical approach, ΔT can be calculated through

$$\Delta Q = \rho V \int_{RT}^{T} c_p dT \qquad (4)$$

where ρ is the film density[45], c_p the specific heat, V the heated volume, and ΔQ the overall energy absorbed per laser pulse (Table I). This approach allows us to predict an average temperature increase $\Delta T \cong 300$ K, per pulse, of the heated volume (see Supplemental Material[32] paragraphs II and III for a detailed discussion). Consequently, α_L can be calculated for our CSL sample from equation 4, which results a factor $\sim$2.5 higher than the GST_{225} case (both values are reported in Table II). This implies that, at least during the fast thermal quenching, the CSL structure is softer (higher α_L) then the bulk case.

Finally, it is important to underly that the extrapolated value of ΔT, for time delays below 150 ps (Fig. 2(d)), does not exceed the melting temperature of the superlattice[46]. Combining this finding with the experimental observation that no phase transformation (e.g. melting) is observed by means of tr-XAS, we demonstrate that ultrafast optical overheating is a reversible process at this laser fluence regime and photon energy.

IV. CONCLUSIONS

In conclusion, the dynamics of the Ge-Te local atomic structure in a CSL, during the free cooling phase of an

	CSL (this work)		references
τ_0	255	ps	
α_L	6 10^{-5}	K^{-1}	2.44 10^{-5} GST_{225}[42,43]
$\delta\sigma$	2%	$\frac{\Delta L}{L}$	
$\Delta T_{/pulse}$	$\sim$ 300	K	
$\frac{\Delta T}{\tau_0}$	$\sim 10^{12}$	K/s	ref.[36] (p. 261)[37,38]

TABLE II: Thermoelastic parameters of the out-of-equilibrium CSL

ultrafast heating - fast cooling cycle is revealed by time resolved XAS and first-principle theory modelling.

In addition to probing the atomic local structure, our approach reveals the significant impact of the lattice strain on the strength of bonds between atoms, from which strongly depends the quenching dynamics and, for example, the melting kinetics of a solid.

Our method is used here to (i) interpret the observed XAS spectral changes in terms of a dynamical microstructural picture of the Ge 4sp-bonding relaxation and (ii) estimate relevant elastic properties of the out-of-equilibrium state of the CSL film.

Futhermore, by combining thermoelastic considerations and a microscopic multiple scattering approach we establish a direct connection between the structural microscopic evolution and the dielectric response in a CSL,

which is fundamental for developing a microscopic theory for ultrafast phase transition and ultimately design new PCMs with improved performances.

All together these results can open the route for future studies aimed to clarify the role of a transient structural strain on the strength of bonds between atoms in phase change materials in the proximity or even during a phase transition.

V.   ACKNOWLEDGMENTS

* marco.malvestuto@elettra.eu
[1] M. Wuttig and N. Yamada, Nature Materials **6**, 824 (2007).
[2] M. H. R. Lankhorst, B. W. S. M. M. Ketelaars, and R. A. M. Wolters, Nature Materials **4**, 347 (2005).
[3] J. Tominaga, P. Fons, A. Kolobov, T. Shima, T. C. Chong, R. Zhao, H. K. Lee, and L. Shi, Japanese Journal of Applied Physics **47**, 5763 (2008).
[4] R. Simpson, P. Fons, A. Kolobov, T. Fukaya, M. Krbal, T. Yagi, and J. Tominaga, Nature Nanotechnology **6**, 501 (2011).
[5] D. A. Baker, M. A. Paesler, G. Lucovsky, S. C. Agarwal, and Taylor, P.C., Physical Review Letters **96**, 255501 (2006).
[6] X. Yu and J. Robertson, Scientific Reports **5**, 12612 (2015).
[7] Z. Sun, J. Zhou, and R. Ahuja, Physical Review Letters **96**, 055507 (2006).
[8] W. Wełnic, S. Botti, L. Reining, and M. Wuttig, Physical Review Letters **98**, 236403 (2007).
[9] Z. Sun, J. Zhou, and R. Ahuja, Physical Review Letters **98**, 055505 (2007).
[10] A. Klein, H. Dieker, B. Späth, P. Fons, and A. Kolobov, Physical Review (2008), 10.1103/PhysRevLett.100.016402.
[11] S. Caravati, M. Bernasconi, T. D. Kühne, M. Krack, and M. Parrinello, Physical Review Letters **102**, 205502 (2009).
[12] S. H. Lee and H. K. Henisch, Journal of Non-Crystalline Solids **11**, 192 (1972).
[13] K. W. Böer and S. R. Ovshinsky, Journal of Applied Physics **41**, 2675 (1970).
[14] K. Makino, J. Tominaga, A. V. Kolobov, P. Fons, and M. Hase, Applied Physics Letters **101**, 232101 (2012).
[15] L. Waldecker, T. A. Miller, M. Rude, R. Bertoni, and J. Osmond, Nature Materials **14**, 991 (2015).
[16] K. V. Mitrofanov, P. Fons, K. Makino, R. Terashima, T. Shimada, A. V. Kolobov, J. Tominaga, V. Bragaglia, A. Giussani, R. Calarco, H. Riechert, T. Sato, T. Katayama, K. Ogawa, T. Togashi, M. Yabashi, S. Wall, D. Brewe, and M. Hase, Nature Publishing Group **6**, 20633 (2016).
[17] M. Le Gallo, A. Athmanathan, D. Krebs, and A. Sebastian, Journal of Applied Physics **119**, 025704 (2016).
[18] G. Bruns, P. Merkelbach, C. Schlockermann, M. Salinga, M. Wuttig, T. D. Happ, J. B. Philipp, and M. Kund, Applied Physics Letters **95**, 043108 (2009).
[19] D. Krebs, S. Raoux, C. T. Rettner, G. W. Burr, M. Salinga, and M. Wuttig, Applied Physics Letters **95**, 082101 (2009).
[20] K. Kohary and C. D. Wright, Applied Physics Letters **98**, 223102 (2011).
[21] J. A. Vázquez Diosdado, P. Ashwin, K. I. Kohary, and C. D. Wright, Applied Physics Letters **100**, 253105 (2012).
[22] L. Cao, L. Wu, W. Zhu, X. Ji, Y. Zheng, Z. Song, F. Rao, S. Song, Z. Ma, and L. Xu, Applied Physics Letters **107**, 242101 (2015).
[23] X. Zhou, J. Kalikka, X. Ji, L. Wu, Z. Song, and R. E. Simpson, Advanced materials (Deerfield Beach, Fla.) **28**, 3007 (2016).
[24] W. Gawelda, J. Siegel, C. N. Afonso, V. Plausinaitiene, A. Abrutis, and C. Wiemer, Journal of Applied Physics **109**, 123102 (2011).
[25] M. Krbal, A. Kolobov, P. Fons, J. Tominaga, S. R. Elliott, J. Hegedüs, and T. Uruga, Physical Review B - Condensed Matter and Materials Physics **83**, 054203 (2011).
[26] M. Krbal, A. Kolobov, P. Fons, K. V. Mitrofanov, Y. Tamenori, J. Hegedüs, S. R. Elliott, and J. Tominaga, Applied Physics Letters **102**, 111904 (2013).
[27] P. Castrucci, R. Gunnella, M. D. Crescenzi, M. Sacchi, G. Dufour, and F. Rochet, Physical Review B **60**, 5759 (1999).
[28] B. Casarin, A. Caretta, J. Momand, B. J. Kooi, M. A. Verheijen, V. Bragaglia, R. Calarco, M. Chukalina, X. Yu, J. Robertson, F. R. L. Lange, M. Wuttig, A. Redaelli, E. Varesi, F. Parmigiani, and M. Malvestuto, Scientific Reports **6**, 22353 (2016).
[29] J. Momand, R. Wang, J. Boschker, M. A. Verheijen, R. Calarco, and B. J. Kooi, Nanoscale **7**, 19136 (2015).
[30] L. Stebel, M. Malvestuto, V. Capogrosso, P. Sigalotti, B. Ressel, F. Bondino, E. Magnano, G. Cautero, and F. Parmigiani, Review of Scientific Instruments **82**, 123109 (2011).
[31] A. Caretta, B. Casarin, P. Di Pietro, A. Perucchi, S. Lupi, V. Bragaglia, R. Calarco, F. R. L. Lange, M. Wuttig, F. Parmigiani, and M. Malvestuto, Physical Review B **94**, 045319 (2016).

[32] See Supplemental Material at [URL will be inserted by publisher] for detailed discussion and calculations.

[33] P. Fons, P. Rodenbach, K. V. Mitrofanov, and A. Kolobov, Physical Review B **90**, 094305 (2014).

[34] P. Fons, H. Osawa, A. Kolobov, T. Fukaya, M. Suzuki, T. Uruga, N. Kawamura, H. Tanida, and J. Tominaga, Physical Review B **82**, 041203 (2010).

[35] http://henke.lbl.gov/optical_constants/filter2.html (accessed December 7, 2015).

[36] Raoux, S and Wuttig, M, *Phase change materials*, edited by S. Raoux and M. Wuttig, science and applications (Springer, 2010).

[37] P. Jund, D. Caprion, and R. Jullien, Physical Review Letters **79**, 91 (1997).

[38] J. Hegedüs and S. R. Elliott, Nature Materials **7**, 399 (2008).

[39] J. J. Rehr, J. J. Kas, M. P. Prange, A. Sorini, Y. Takimoto, and F. Vila, Comptes Rendus Physique **10**, 548 (2009).

[40] J. J. Rehr, J. J. Kas, F. D. Vila, M. P. Prange, and K. Jorissen, Physical Chemistry Chemical Physics **12**, 5503 (2010).

[41] C. Thomsen, H. T. Grahn, H. J. Maris, and J. Tauc, Physical Review B **34**, 4129 (1986).

[42] I. M. Park, J. K. Jung, S. O. Ryu, K. J. Choi, B. G. Yu, Y. B. Park, S. M. Han, and Y. C. Joo, Thin Solid Films **517**, 848 (2008).

[43] J. Kalb, F. Spaepen, T. P. Leervad Pedersen, and M. Wuttig, Journal of Applied Physics **94**, 4908 (2003).

[44] G. Eesley, Physical Review B **33**, 2144 (1986).

[45] J. L. Battaglia, A. Kusiak, V. Schick, A. Cappella, C. Wiemer, M. Longo, and E. Varesi, Journal of Applied Physics **107**, 044314 (2010).

[46] N. Yamada, E. Ohno, K. Nishiuchi, N. Akahira, and M. Takao, Journal of Applied Physics **69**, 2849 (1991).